

# THE ROLE OF ICE COMPOSITIONS AND MORPHOLOGY FOR SNOWLINES AND THE C/N/O RATIOS IN ACTIVE DISKS

ANA-MARIA A. PISO<sup>1</sup>, KARIN I. ÖBERG<sup>1</sup>, JAMILA PEGUES<sup>2</sup>

*Draft version December 14, 2015*

## ABSTRACT

The elemental compositions of planets define their chemistry, and could potentially be used as beacons for their formation location if the elemental gas and grain ratios of planet birth environments, i.e. protoplanetary disks, are well understood. In disks, the ratios of volatile elements, such as C/O and N/O, are regulated by the abundance of the main C, N, O carriers, the ice environment in which these carriers reside, and the presence of snowlines of major volatiles at different distances from the central star. We explore the effects of dynamical processes, molecular compositions and abundances, and the ice morphology of dust grains in disks on the snowline locations of the main C, O and N carriers, and their consequences for the C/N/O ratio in gas and dust throughout the disk. We find that radial drift and accretion alone can reduce the snowline radii of the main C, O and N carriers, i.e. H<sub>2</sub>O, CO<sub>2</sub>, CO and N<sub>2</sub>, by 40-60% compared to static disks. If CO and N<sub>2</sub> are bound to water ice instead of pure ices, their snowlines move inward by  $\sim 70\%$ . Both of these effects substantially change the disk regions where C/O and N/O are enhanced over the stellar value. In the outer disk, the gaseous C/O and N/O are enhanced by factors of  $\sim 2$  and  $\sim 3$ , respectively. Our estimates for the C/N/O ratios are only modestly affected by the presence of some C in the form of CH<sub>4</sub> and of some N in the form of NH<sub>3</sub>.

## 1. INTRODUCTION

*Background info. Importance of volatiles in disks and planetary atmospheres, detections of snowlines in disks, C/O ratios etc. State again the importance of radial drift and gas accretion on the snowline locations, and that a systematic study of the combination of these two particular effects across the disk has not been done before. Then transition to the fact that we provide such a systematic study in Paper I and in this paper. Here, we expand the model of Paper I by making three additions: (1) we add N and CH<sub>4</sub> in the static chemistry model, and explore how different abundances of CH<sub>4</sub> and of the N main carriers (N<sub>2</sub> and NH<sub>3</sub>) affect the C/O and N/O ratios, (2) we quantify the effect of radial drift and gas accretion on the N<sub>2</sub>, CH<sub>4</sub> and NH<sub>3</sub> snowline locations, and (3) we explore how different binding energies of CO and N<sub>2</sub> affect their snowline locations.*

## 2. COUPLED DRIFT-DESORPTION MODEL REVIEW

We begin with a brief review of Paper I's model for the effect of radial drift and viscous gas accretion on volatile snowline locations. We review our disk model in Section 2.1, and summarize our numerical method and results in Section 2.2.

### 2.1. Disk Model

We first assume a static disk, which is only irradiated by the central star and does not experience redistribution of solids or radial movement of the nebular gas. To quantify the effects of radial drift and gas accretion, we use a viscous disk with a spatially and temporally constant mass flux,  $\dot{M}$ . The viscous disk takes into account

radial drift, gas accretion onto the central star, as well as accretion heating. We prefer this disk model to an irradiated or evolving disk (see Paper I) because it includes all the dynamical and thermal processes we are interested in for the scope of this paper, and therefore it is the most realistic one.

We model the static disk as a minimum mass solar nebula (MMSN), using a prescription for the gas surface density,  $\Sigma$ , and disk midplane temperature,  $T$ , similar to that of Chiang & Youdin (2010):

$$\Sigma = 2000 (r/\text{AU})^{-1} \text{ g cm}^{-2} \quad (1a)$$

$$T = 120 (r/\text{AU})^{-3/7} \text{ K}, \quad (1b)$$

where  $r$  is the semimajor axis. Based on observations of protoplanetary disks (Andrews et al. 2010), we choose a flatter surface density than the one assumed by Chiang & Youdin (2010), where  $\Sigma \propto r^{-3/2}$ .

We use the Shakura & Sunyaev (1973) steady-state disk solution to model the viscous disk. Solving the Equation set of Appendix A in Paper I yields an expression for the temperature profile in a steady-state disk:

$$T_{\text{act}} = \frac{1}{4r} \left( \frac{3G\kappa_0 \dot{M}^2 M_* \mu m_p \Omega_k}{\pi^2 \alpha k_B \sigma} \right)^{1/3}. \quad (2)$$

Here  $G$  is the gravitational constant,  $\kappa_0 = 2 \times 10^{-6}$  is a dimensionless coefficient in the opacity law  $\kappa = \kappa_0 T_{\text{act}}^2$ ,  $M_* = M_\odot$  is the mass of the central star,  $\mu = 2.35$  is the mean molecular weight of the nebular gas,  $m_p$  is the proton mass,  $\Omega_k = \sqrt{GM_\odot}/r^3$  is the Keplerian angular velocity,  $\alpha = 0.01$  is a dimensionless coefficient (see below for details),  $k_B$  is the Boltzmann constant, and  $\sigma$  is the Stefan-Boltzmann constant. The final midplane temperature profile is computed as

$$T^4 = T_{\text{act}}^4 + T_{\text{irr}}^4, \quad (3)$$

<sup>1</sup> Harvard-Smithsonian Center for Astrophysics, 60 Garden Street, Cambridge, MA 02138

<sup>2</sup> Department of Astrophysical Sciences, Princeton University

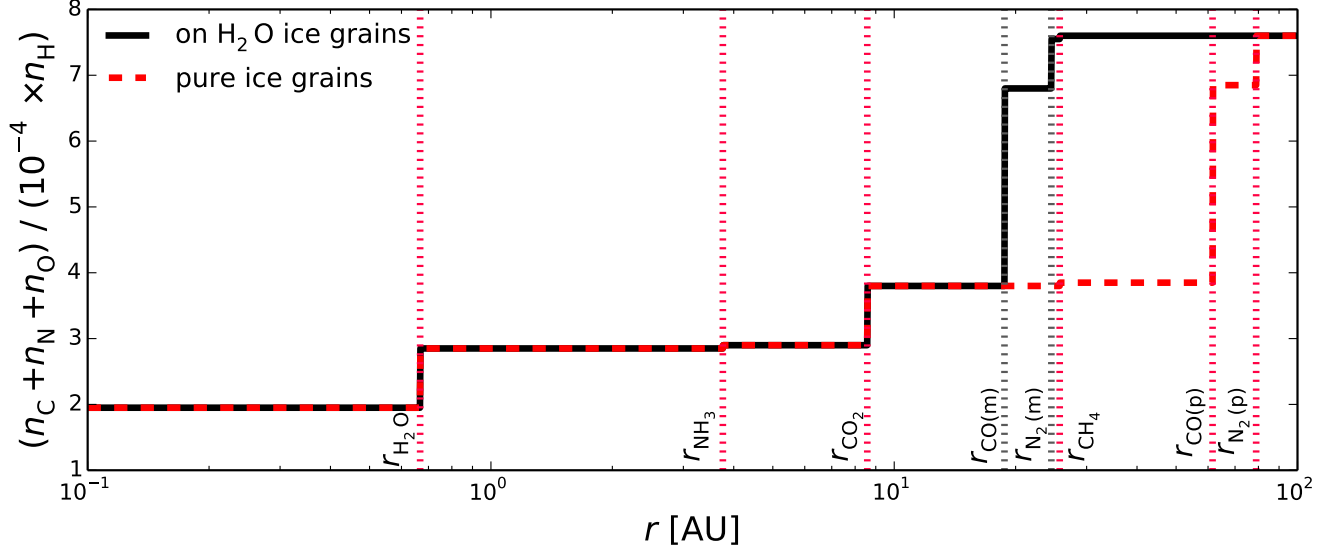


FIG. 1.— CNO abundance in grains...

where  $T_{\text{irr}} = T$  from Equation (1b). We use this expression because in addition to accretion heating, stellar irradiation also contributes to the disk thermal structure.

The steady-state disk has an  $\alpha$ -viscosity prescription, where the kinematic viscosity is  $\mu = \alpha c H$ . Here  $c \equiv \sqrt{k_B T / (\mu m_p)}$  is the isothermal sound speed (with  $T$  from Equation 3), and  $H \equiv c / \Omega_k$  is the disk scale height. We can then determine the gas surface density for a viscous disk as (Shakura & Sunyaev 1973; see also Paper I for a more detailed explanation of these calculations):

$$\Sigma = \frac{\dot{M}}{3\pi\nu}. \quad (4)$$

We choose  $\dot{M} = 10^{-8} M_\odot \text{ yr}^{-1}$ , consistent with mass flux observations in disks (e.g., Andrews et al. 2010). As acknowledged in Paper I, the mass flux rate  $\dot{M}$  and stellar luminosity  $L_*$  will vary throughout the disk lifetime (Kennedy et al. 2006, Chambers 2009), in contrast with our simplified model which assumes that both quantities are constant. This effect will be most pronounced in the inner disk ( $\lesssim$  few AU), where accretion heating dominates. We thus acknowledge that the location of the  $\text{H}_2\text{O}$  snowline may be determined by the decline in  $\dot{M}$  or  $L_*$  with time, rather than radial drift (see Paper I, Section 2.1 for a more detailed explanation).

## 2.2. Desorption-Drift Equations and Results

For a range of initial icy grain sizes composed of a single volatile, we showed in Paper I that the timescale on which these particles desorb is comparable to their radial drift time, as well as to the accretion timescale of the nebular gas onto the central star. We thus have to take into account both drift and gas accretion when we calculate the disk location at which a particle desorbs, since that location may be different from the snowline position in a static disk for a given volatile (see Figure 1 and Öberg et al. 2011b). We determine a particle's final location in the disk by solving the following coupled

differential equations:

$$\frac{ds}{dt} = -\frac{3\mu_x m_p}{\rho_s} N_x R_{\text{des},x} \quad (5a)$$

$$\frac{dr}{dt} = \dot{r}, \quad (5b)$$

where  $s$  is the particle size,  $t$  is time,  $\mu_x$  is the mean molecular weight of volatile  $x$ ,  $\rho_s = 2 \text{ g cm}^{-3}$  is the density of an icy particle,  $N_x \approx 10^{15} \text{ sites cm}^{-2}$  is the number of adsorption sites of molecule  $x$  per  $\text{cm}^{-2}$ ,  $R_{\text{des},x}$  is the desorption rate of species  $x$ , and  $\dot{r}$  is the particle's radial drift velocity. We calculate  $R_{\text{des}}$  and  $\dot{r}$  as follows.

The desorption rate  $R_{\text{des},x}$  (per molecule) is (Hollenbach et al. 2009)

$$R_{\text{des},x} = \nu_x \exp(-E_x / T_{\text{grain}}), \quad (6)$$

where  $E_x$  is the adsorption binding energy in units of Kelvin,  $T_{\text{grain}} = T$  is the grain temperature (assumed to be the same as the disk temperature, see Paper I), and  $\nu_x = 1.6 \times 10^{11} \sqrt{(E_x / \mu_x)} \text{ s}^{-1}$  is the molecule's vibrational frequency in the surface potential well. We discuss our choices for  $E_x$  for the different volatile species in Sections 3 and 4.

Following Chiang & Youdin (2010) and Birnstiel et al. (2012), a particle's radial drift velocity can be approximated as

$$\dot{r} \approx -2\eta\Omega_k r \left( \frac{\tau_s}{1 + \tau_s^2} \right) + \frac{\dot{r}_{\text{gas}}}{1 + \tau_s^2}, \quad (7)$$

where the first term is the drift velocity in a non-accreting disk and the second term accounts for the radial movement of the gas. Here  $\eta \approx c^2 / (2v_k^2)$ , where  $v_k$  is the Keplerian velocity, and  $\tau_s \equiv \Omega_k t_s$  is the dimensionless stopping time:

$$t_s = \begin{cases} \rho_s s / (\rho c), & s < 9\lambda/4 \text{ Epstein drag} \\ 4\rho_s s^2 / (9\rho c \lambda), & s < 9\lambda/4, \text{Re} \lesssim 1 \text{ Stokes drag,} \end{cases} \quad (8)$$

where  $\rho$  is the disk mid-plane density,  $\lambda$  is the mean free path and  $\text{Re}$  is the Reynolds number. The gas accretion velocity  $\dot{r}_{\text{gas}}$  is determined from  $\dot{M} = -2\pi r \dot{r}_{\text{gas}} \Sigma$ , for a fixed  $\dot{M}$  and with  $\Sigma$  given by Equation (4).

For a particle of initial size  $s_0$ , we solve the Equation set (5) with the initial conditions  $s(t_0) = s_0$  and  $r(t_0) = r_0$ , where  $t_0$  is the time at which we start the integration and  $r_0$  is the particle's initial location. We stop our simulation after  $t_d = 3$  Myr, the disk lifetime, since this is roughly the timescale on which planets form ( ), and determine the desorption timescale  $t_{\text{des}}$  from  $s(t_{\text{des}}) = 0$ , and thus a particle's desorption distance  $r_{\text{des}} = r(t_{\text{des}})$ . Our results are insensitive to our choice of  $t_0$  as long as  $t_0 \ll t_d$ . We note that a particle's size is initially fixed and only changes due to desorption. We thus do not take into account processes such as grain coagulation or fragmentation, which nonetheless occur in disks (e.g., Birnstiel et al. 2012, Pérez et al. 2012). We discuss the effect of these processes on snowline locations in Paper I.

As we show in Paper I, a particle of initial size  $s_0$  can experience three outcomes after  $t_d = 3$  Myr: (1) it can remain at its initial location, (2) it can drift towards the host star, then stop without evaporating significantly, and (3) it can completely desorb on a timescale shorter than 3 Myr. Particles in scenarios (1) and (2) are thus not affected by radial drift or gas accretion, and the snowline locations are those for a static disk. In contrast, the grains in case (3) desorb *instantaneously* and *at a fixed particle-size dependent location* in the disk, regardless of their initial position. The snowline locations for these particles will thus be fixed for a given initial particle size and disk model. We have found that grains with sizes  $\sim 0.001 \text{ cm} \lesssim s \lesssim 7$  satisfy this condition for our fiducial disk.

### 3. CH<sub>4</sub> AND C/O RATIOS

Both in Solar system comets and in protoplanetary disks, carbon and oxygen are primarily contained in H<sub>2</sub>O, CO<sub>2</sub> and CO (e.g., Rodgers & Charnley 2002, Lodders 2003, Pontoppidan 2006). However, some fraction of the carbon abundance may also be carried by CH<sub>4</sub> (e.g., Mumma et al. 1996), which may change the C/O ratio in gas and in dust throughout the disk. To quantify the magnitude of this effect, we use measured CH<sub>4</sub> abundances in protostellar cores from the *Spitzer* c2d Legacy ice survey (Evans et al. 2003). We explore the parameter space of possible CH<sub>4</sub> abundances by assuming three different scenarios: (1) no CH<sub>4</sub>, (2) the median CH<sub>4</sub> observed abundance (hereafter CH<sub>4</sub>-mid), and (3) the maximum CH<sub>4</sub> observed abundance (hereafter CH<sub>4</sub>-max). Thus  $n_{\text{CH}_4\text{-mid}} = 0.0555 \times n_{\text{H}_2\text{O}}$  (Öberg et al. 2011a) and  $n_{\text{CH}_4\text{-mid}} = 0.13 \times n_{\text{H}_2\text{O}}$  (Öberg et al. 2008). Similarly to Paper I, we use the H<sub>2</sub>O, CO<sub>2</sub> and CO abundances of Öberg et al. (2011b). Since the abundance of carbon grains is uncertain, we assume that all the carbon that is not in the form of CH<sub>4</sub> is found in carbon grains, so that we reproduce the Solar C/O ratio (gas+dust) of 0.54.

We determine the location of the H<sub>2</sub>O, CO<sub>2</sub>, CO and CH<sub>4</sub> snowlines in our static disk by balancing desorption with readsorption, following Hollenbach et al. (2009). The binding energies of H<sub>2</sub>O, CO<sub>2</sub>, CO and CH<sub>4</sub> as pure

ices are 5800 K, 2000 K, 1388 K and 1300 K, respectively (Fraser et al. 2001, Collings et al. 2004, Fayolle et al., submitted, Garrod & Herbst 2006).

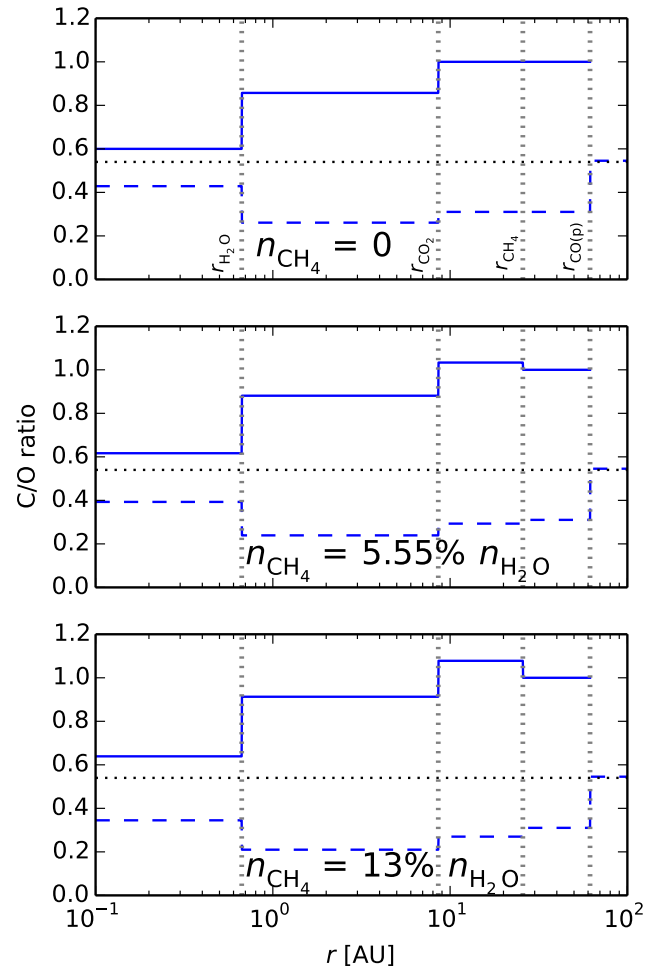


FIG. 2.— C/O ratio in a static disk for different CH<sub>4</sub> abundances and CO binding energies...

Figure 2 shows the C/O ratio in gas and dust as a function of semimajor axis in a static disk, for different CH<sub>4</sub> abundances as outlined above. As in Öberg et al. (2011b) and Paper I, a gaseous C/O ratio of unity can be achieved beyond the CO<sub>2</sub> snowline, where oxygen gas is significantly depleted (top panel). The gas-phase C/O ratio may be further enhanced between the CO<sub>2</sub> and CH<sub>4</sub> snowlines due to the presence of additional carbon gas from CH<sub>4</sub>. In this region, the C/O ratio increases by 3% for CH<sub>4</sub>-mid and by 8% for CH<sub>4</sub>-max, as displayed in the middle and bottom panel of Figure 2. Based on current observations of CH<sub>4</sub> abundances, its presence in the disk only modestly affects the C/O ratio. Given the larger uncertainties in overall volatile abundances, we can neglect CH<sub>4</sub> when estimating the C/O ratio in static disks.

As noted in Section 1, the CO binding energy varies significantly depending on the environment in which the icy grains reside. If CO ice is layered on top of a water ice substrate, its binding energy will be larger than in the pure ice case (1388 K) due to the higher H<sub>2</sub>O binding en-

ergy. Fayolle et al. (submitted) find a CO binding energy of 834 K in the layered ice scenario. We use the model of Section 2 to estimate the movement of the CO snowline for different grain morphologies in a viscous disk.

Figure 3 shows the  $\text{H}_2\text{O}$ ,  $\text{CO}_2$  and CO snowline locations for particles with initial sizes  $\sim 0.06 \text{ cm} \lesssim s \lesssim 7 \text{ m}$  as well as estimates for the C/O ratio in gas and dust in a viscous disk, with the CO snowline calculated under different grain morphologies as noted above. The true snowline for particles that desorb outside the static snowline is the static snowline itself, hence desorbing particles with  $s < 0.06 \text{ cm}$  do not form true snowlines. As calculated in Paper I, drift and gas accretion may move the snowlines inwards by up to 40-60% compared to a static disk, and specifically by up to  $\sim 50\%$  in the case of the CO snowline. This result is preserved for the updated CO binding energies, both for pure ice and on a water ice substrate. However, a layered grain structure moves the CO snowline inwards significantly: for our fiducial disk model,  $r_{\text{CO,layered}} \approx 8.7 \text{ AU}$ . Thus if CO is bound to water ice instead of pure ices, the CO snowline may move inward by up to 70%. This large inward movement of the CO snowline implies that C/O ratios of order unity may be reached much closer to the host star if CO is layered on a water ice substrate, and may be inside 10 AU for certain disk parameters.

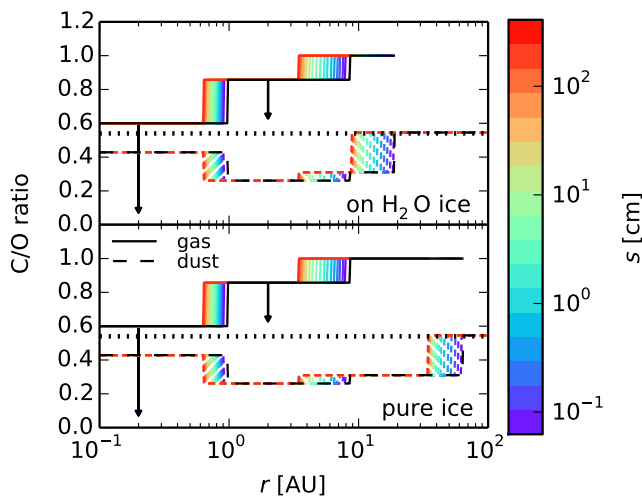


FIG. 3.— C/O ratio as function of semimajor axis for CO combined with  $\text{H}_2\text{O}$  (top panel) and pure CO ice (bottom panel).... Drift and gas accretion move the CO snowlines inward by x% and y%, respectively.

#### 4. NITROGEN CARRIERS AND N/O RATIOS

Similar to the previous section, but with more details. Discuss that nitrogen is abundant in the solar system and disks and primarily found as  $\text{N}_2$ . Due to the high volatility of  $\text{N}_2$ , the gas phase N/O ratio in the outer disk may be even more enhanced than the C/O ratio. A fraction of the nitrogen abundance may be also carried by  $\text{NH}_3$ . Discuss  $\text{NH}_3$  observed abundances and the choices that we make (no  $\text{NH}_3$ , median, maximum). State that the  $\text{NH}_3$  desorption energy is only weakly dependent on whether it's pure  $\text{NH}_3$  or combined with  $\text{H}_2\text{O}$ , but that is not the case for  $\text{N}_2$ . Present new binding energies for  $\text{N}_2$  as pure ice and combined with water. Show Figure 4 and discuss how different nitrogen abundances and binding energies affect snowline locations and N/O ratio:  $\text{N}_2$  combined with  $\text{H}_2\text{O}$  moves the  $\text{N}_2$  snowline inward by  $\sim 50 \text{ AU}$  (will calculate percentages too); the maximum reasonable abundance of  $\text{NH}_3$  changes the N/O ratio by  $\sim 15\%$ . In the outer disk, the N/O ratio is enhanced by a factor of  $\sim 4$  compared to the solar value, twice as much as the C/O enhancement. Show Figure 5 and quantify the effect of drift and accretion on the  $\text{NH}_3$  snowline compared to a static disk. While  $\text{NH}_3$  does not have a significant effect on the N/O ratio in a static disk, this effect may be larger in a viscous disk, as the N gas abundance inside the  $\text{NH}_3$  snowline may be enhanced due to the differential motion of the desorbed ices and overall nebular gas (refer to Paper I). In this study, however, we neglect these effects and therefore do not include  $\text{NH}_3$  in estimating the N/O ratio (again, N/O ratio figure with drift is quite messy when including  $\text{NH}_3$  and does not add any information that is not already shown in Figures 4 and 5). Show Figure 6 and estimate the difference between  $\text{N}_2$ - $\text{H}_2\text{O}$  and  $\text{N}_2$  pure ice snowlines in the case of drift, as well as the comparisons for the static disk for the  $\text{N}_2$  snowline. State that there will be an overabundance of gas-phase N/O between the CO and  $\text{N}_2$  snowlines, as there is no oxygen gas in this region.

#### 5. DISCUSSION

Discuss how entrapment of volatiles by  $\text{H}_2\text{O}$  affects volatile abundances and C/O ratios. Re-emphasize the fact that the C/O and N/O ratios are upper estimates, and that  $\text{CH}_4$  and  $\text{NH}_3$  might matter in a viscous disk. State that we plan to address this in a future paper. More TBD.

#### 6. SUMMARY

Maybe we can include the summary in the discussion section?

#### REFERENCES

- Andrews, S. M., Wilner, D. J., Hughes, A. M., Qi, C., & Dullemond, C. P. 2010, *ApJ*, 723, 1241  
 Birnstiel, T., Klahr, H., & Ercolano, B. 2012, *A&A*, 539, A148  
 Chambers, J. E. 2009, *ApJ*, 705, 1206  
 Chiang, E., & Youdin, A. N. 2010, *Annual Review of Earth and Planetary Sciences*, 38, 493  
 Collings, M. P., Anderson, M. A., Chen, R., et al. 2004, *MNRAS*, 354, 1133  
 Evans, II, N. J., Allen, L. E., Blake, G. A., et al. 2003, *PASP*, 115, 965  
 Fraser, H. J., Collings, M. P., McCoustra, M. R. S., & Williams, D. A. 2001, *MNRAS*, 327, 1165  
 Garrod, R. T., & Herbst, E. 2006, *A&A*, 457, 927  
 Hollenbach, D., Kaufman, M. J., Bergin, E. A., & Melnick, G. J. 2009, *ApJ*, 690, 1497  
 Kennedy, G. M., Kenyon, S. J., & Bromley, B. C. 2006, *ApJ*, 650, L139  
 Lodders, K. 2003, *ApJ*, 591, 1220  
 Mumma, M. J., Disanti, M. A., dello Russo, N., et al. 1996, *Science*, 272, 1310  
 Öberg, K. I., Boogert, A. C. A., Pontoppidan, K. M., et al. 2008, *ApJ*, 678, 1032  
 —. 2011a, *ApJ*, 740, 109  
 Öberg, K. I., Murray-Clay, R., & Bergin, E. A. 2011b, *ApJ*, 743, L16

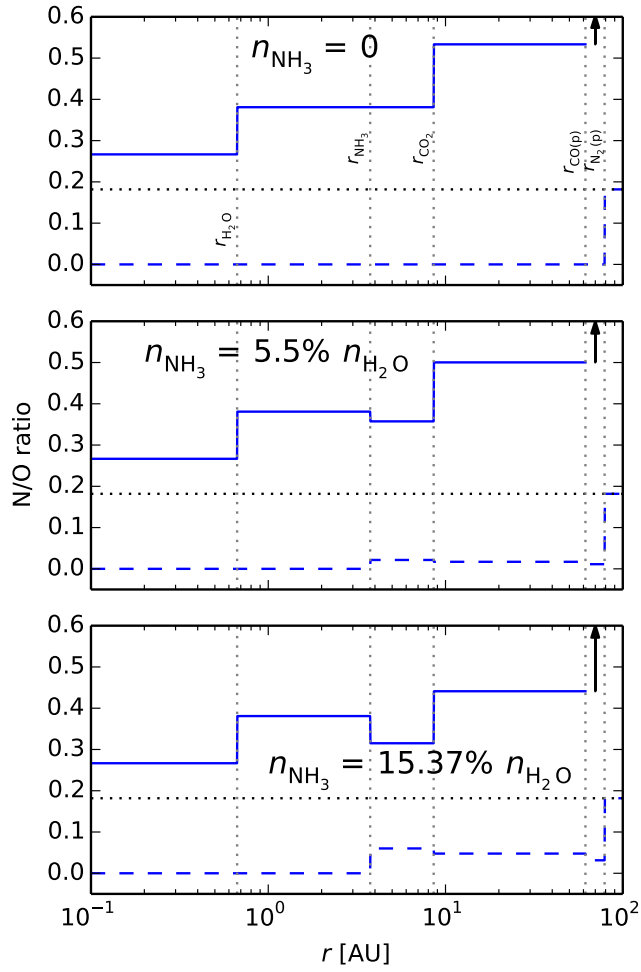


FIG. 4.— N/O ratio in a static disk for different NH<sub>3</sub> abundances and N<sub>2</sub> binding energies...

Pérez, L. M., Carpenter, J. M., Chandler, C. J., et al. 2012, ApJ, 760, L17  
 Pontoppidan, K. M. 2006, A&A, 453, L47  
 Rodgers, S. D., & Charnley, S. B. 2002, MNRAS, 330, 660  
 Shakura, N. I., & Sunyaev, R. A. 1973, A&A, 24, 337

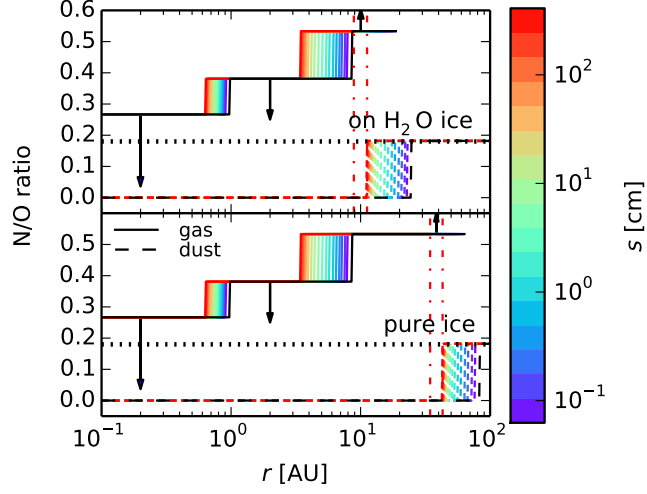


FIG. 5.— N/O ratio as function of semimajor axis for N<sub>2</sub> combined with H<sub>2</sub>O (top panel) and pure N<sub>2</sub> ice (bottom panel).... Drift and gas accretion move the N<sub>2</sub> snowlines inward by  $x\%$  and  $y\%$ , respectively. Overabundance of gas-phase N/O between the CO and N<sub>2</sub> snowlines, marked by the vertical red dash-dotted lines for the largest drifting particles in our model.